Progress In Electromagnetics Research M, Vol. 81, 55–66, 2019

Broadbeam Coplanar-Parasitic Rectangular Dielectric Resonator Antenna

Syeda Hiba Hussain Mashhadi[1, *], Muhammad Wasif Niaz[1], Yong-Chang Jiao[2], and Jingdong Chen[1]

Abstract—A novel broadbeam aperture-coupled coplanar parasitic rectangular dielectric resonator antenna is proposed which yields broadbeam in both working planes simultaneously. The antenna consists of a main radiating rectangular dielectric element centered over a wide feed slot and two parasitic rectangular dielectric elements one on each side of the main radiating element with an optimum gap in between. The dielectric height and wide slot both play an important role in enhancing the beamwidth in two principal planes simultaneously. It is validated that inclusion of parasitic elements enhances the broadbeam bandwidth in addition to frequency bandwidth. First three azimuthal modes are excited out of which first two modes TE^x_{111} and TE^x_{112} are desired. The proposed antenna is compared with single element rectangular dielectric resonator antenna. To validate the proposed design, a prototype is fabricated and measured. The simulated and measured operating frequency bands of the proposed antenna respectively are 4.8 to 6.9 GHz and 5 to 6.8 GHz. The measured E- and H-plane beamwidths range from 115° to 144° and from 115° to 124°, respectively, yielding a wider coverage area.

1. INTRODUCTION

Many recent applications such as GPS (1575.42 MHz, 1227.60 MHz, 1176.45 MHz), telemetry (900 − −928 MHz), and tele-control systems all require an antenna that can provide uniform response over entire upper hemisphere and high gain at low angles. Additionally, safety applications like Adaptive Cruise Control (ACC) and forward collision alert, all use Automotive Radar which needs to have a wide field of view [1]. The latter operates at frequencies above 70 GHz. Microstrip patch antennas (MPA) have so far been used for their attractive features like conformity and low cost. However, for MPAs conductor losses become considerable at millimeter wave frequencies, and they exhibit narrow beam characteristics. Typically, MPAs have E-plane beamwidth of 110° and H-plane beamwidth of 70° and consequently do not comply with the wide beam requirement of above mentioned applications. Dielectric resonator antennas (DRA), however, exhibit no ohmic losses at the mentioned frequency bands [2]. Therefore, DRAs become strong contenders for applications like ACC and forward collision alert where wide beamwidth radar antennas are required. Additionally, a wide beamwidth antenna is also required for GPS, telemetry and tele-control system. Therefore, considering the requirement of prospective applications, there is a dire need of research in the design of broad beamwidth DRAs.

Many solutions for broadening the beamwidth have been proposed for MPAs in the literature such as using artificial electromagnetic materials [2]. A wide beam is achieved in [3] where the dielectric constant of the antenna substrate is artificially modified using arrays of metamaterial inclusions. In [4], the ground of the patch is transformed to a ridge-shaped ground plane to realize wide-beam characteristics. In [5], a composite substrate is used for a microstrip patch antenna to enhance the beamwidth.

Received 1 February 2019, Accepted 26 March 2019, Scheduled 16 May 2019

* Corresponding author: Syeda Hiba Hussain Mashhadi (hiba.mashhadi@mail.nwpu.edu.cn).

[1] Department of Information and Communication Engineering, Northwestern Polytechnical University, Xi'an, Shaanxi 710072, China.

[2] National Key Laboratory of Antennas and Microwave Technology, Xidian University, Xi'an, Shaanxi 710071, China.

There has been a lot of research invested into beamwidth enhancement in microstrip patch antennas. Dielectric resonator antennas (DRA), however, have been investigated for a wide range of attribute improvement like bandwidth enhancement, sidelobe reduction, achieving modal purity, etc. but have not been investigated for broad beamwidth in both working planes simultaneously. Achieving wide beam, one plane is relatively less challenging than aiming for broadbeam radiation patterns in two planes simultaneously. As mentioned above, safety applications operate in millimeter frequency bands, and there is a dire need of research in DRAs in this particular regard since they prove to be better contenders as antennas used for millimeter wave frequency bands. In literature, a meager amount of research can be found on beamwidth enhancement of DRAs in particular and is mentioned as follows. In [6], dielectrics were used to enhance the beamwidth of microstrip patch antenna. In [7–10], techniques such as dielectric loading, carved ground plane, reduced ground plane, and patch loaded DRAs have been used to enhance the beamwidth of DRAs, respectively.

In this paper, beamwidth enhancement method is presented for a DRA. A novel broadbeam copolanar-parasitic rectangular DRA (CoP-RDRA) is proposed which yields broad beam radiation patterns in E- and H-planes simultaneously without utilizing a complex feed mechanism. The novelty of the feed mechanism lies in the fact that a wide feed slot alone excites the two desired modes which are critical to broadside widebeam performance in two planes simultaneously. This is achieved by enhancing the modal resonance bandwidth and merging the two consecutive modes resonances. No additional feed mechanism is required to efficiently couple the two modes, keeping the antenna simple from fabrication view point. However, all the important parameters critical to achieving broad beamwidth in two principal planes simultaneously have been identified, and relations between the wavelength of Mode-I frequency and these parameters have been drawn which give initial values for design dimensions. It is found that parasitic dielectric elements at an optimum gap length from radiating element play an important role in enhancing the beamwidth bandwidth of the antenna and will be shown in the following sections. Here, it is imperative to define the term 'beamwidth bandwidth' as a band of frequencies where the antenna yields broad beamwidth of more than 110° in two planes simultaneously. Single element rectangular dielectric resonator antenna (RDRA) is also designed, and the results are compared with proposed CoP-RDRA in terms of beamwidths in E- and H-planes, beamwidth bandwidth, and radiation pattern stability. The comparisons clearly show that the proposed CoP-RDRA yields wide broadbeam bandwidth with stable radiation patterns and a broadbeam radiation pattern in both principal planes simultaneously.

The paper is organized as follows. In Section 2, the antenna configuration is explained. Design principal and working mechanism based on results from HFSS eigen mode solver are explained in Section 3. Finally in Section 4, antenna performance is discussed in terms of simulated and measured results. Section 5 presents the conclusion.

2. ANTENNA CONFIGURATION

The coplanar parasitic rectangular dielectric resonator antenna is illustrated in Figure 1. The antenna consists of a rectangular dielectric resonator (RDR) radiating element with width $W_{\mathrm{DR}} = 6\,\mathrm{mm}$ and two parasitic elements denoted as PE, placed on two sides of the main radiating element, with width of each being $W_{\mathrm{PE}} = 4\,\mathrm{mm}$. The RDR elements having height $H = 18\,\mathrm{mm}$ and breadth $B = 12\,\mathrm{mm}$ are assembled with 2 mm wide pieces joined t laterally under pressure with an adhesive to achieve the required widths of 6 mm and 4 mm. The dielectric constant of the RDR is chosen to be $\epsilon_{\mathrm{dr}} = 9.8$ and is fed by aperture slot of size $L_s \times W_s$, where $L_s = 0.203\lambda_g$ and $W_s = 0.115\lambda_g$. The slot is excited by a $50\,\Omega$ microstrip feed line of width $W_f = 3.5\,\mathrm{mm}$. The width of microstrip feed line is determined by substrate relative permittivity and thickness. Its length is optimized to match with commercially available $50\,\Omega$ SMA connectors. Several parametric sweeps were run to optimize the slot length and width. The stub of length $st = 0.0785\lambda_g$, starting from the centre of the aperture slot to end of the microstrip line, is used for optimum impedance matching. The substrate used is FR4 with thickness $ts = 2\,\mathrm{mm}$. The optimum substrate size is $L \times L$, where $L = 1.23\lambda_g$. The gap between the radiating and parasitic RDR elements is $g = 0.0535\lambda_g = 3\,\mathrm{mm}$. λ_g is obtained using Mode-I frequency which is 5.34 GHz as computed by HFSS Eigen Mode Solver. The filling material used in the gaps between radiating element and PEs is foam with dielectric constant, $\epsilon_f = 1$ which is equal to that of air. Its

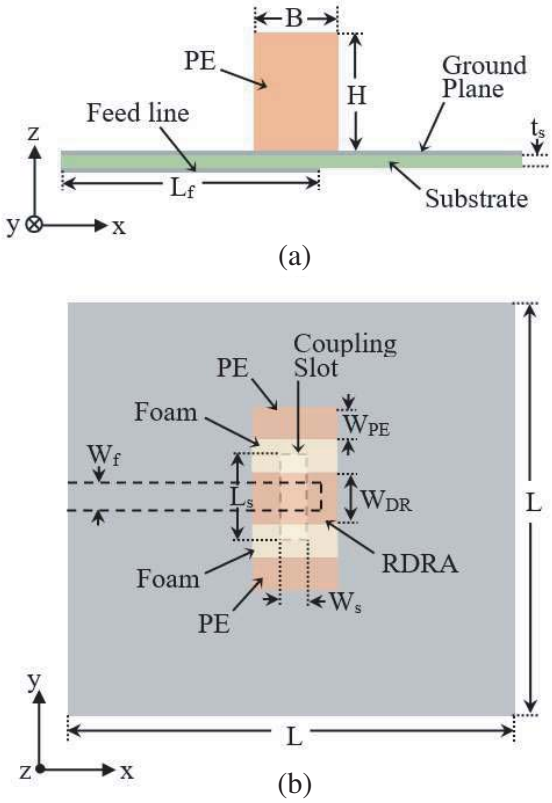

Figure 1. Coplanar-parasitic rectangular dielectric resonator antenna.

width is 3 mm equal to the gap length. This foam helps ensure that the gap length is 3 mm. The effects of air have been considered in the simulations.

3. DESIGN CONCEPT AND MODE ANALYSIS

3.1. Design Concept

The initial values for the dimensions of the rectangular DRA were obtained using the curves given in [11] which plot the normalized frequency F versus the ratio of DRA dimensions d/b for various ratios of a/b where a, b, and d in the reference correspond to B, H, and W (width of RDRA) in this paper. The normalized frequency is defined as:

$$F = \frac{2\pi a f_o \sqrt{\epsilon_r}}{c} \tag{1}$$

For instance, in our case, to solve for a starting value of RDRA resonant frequency with $\epsilon_{\mathrm{dr}} = 9.8$, the dimensions $B = H = W = 12$ mm were used to get $F = 5$, and using the curves, f_o was found to be 6.35 GHz. The dimensions of RDRA, however, later on went through metamorphic transition and were optimized for broadbeam operation. The single element RDRA was fed with an aperture slot. It was found through simulations and experimentation that the antenna yielded broadbeam radiation patterns in two planes simultaneously at a particular height and a wide slot. Simulations showed that as the slot width was increased, modal resonance bandwidth was increased which was critical for achieving wide beam pattern in both planes. RDRA yielded broadbeam in the upper frequency band of Mode-I resonance bandwidth, i.e., the band of frequencies between Mode-I and Mode-II. H and slot dimensions, L_s and W_s were found to have a consistent relation with the Mode-I frequency wavelength named as λ_g. Mode-I frequency was found using HFSS eigen-mode solver which in this case came out to be 5.2 GHz,

and the DR height H was 18 mm = $0.315\lambda_g$. This was done for single element RDRA which yielded broadbeam in two principal planes at very narrow band of frequencies. However, this initial work paved the way and formed a basis for the design of CoP-RDRA. These results will be presented and discussed in detail in the following discussion.

Moving on to the design of CoP-RDRA, we start with a well established fact that introducing air gaps in the DR tends to enhance the impedance bandwidth of the antenna. We applied the same principle and attempted to increase the *beamwidth bandwidth* of the DRA since introducing gaps to enhance beamwidth-bandwidth has not been reported in the literature. Horizontal gaps usually increase the impedance bandwidth; however, the same approach did not help enhance the beamwidth bandwidth. Therefore, vertical gaps were introduced. Then, we used HFSS eigen mode solver to identify the modal frequencies of the isolated RDR with vertical gaps. This gives us initial values for important parameters like dielectric resonator (DR) height, H, gap length, g, DR radiating element width, W_{DR}, and DR parasitic element width, W_{PE} in terms of Mode-I frequency wavelength. Here, it is imperative to mention that the initial calculations carried out for single element RDRA played an important role in setting the initial dimensions for CoP-RDR.

Figure 2 presents the variation of mode frequencies with varying height H for a CoP-RDR. As can be seen from Figure 2, there is no variation in Mode-I frequency with changing dielectric resonator height H. The plot points towards an important trait that the antenna yields broadbeam in two planes at frequencies between Mode-I and Mode-II resonances. Therefore, Mode-I frequency provides an initial marker for successfully identifying the broadbeam frequencies. The next step will be to specify the DR height optimum for broadbeam operation. However, using the calculation for single element RDR, the optimum height has already been pointed out to be 18 mm, and the antenna dimensions have a consistent relation with Mode-I frequency wavelength because it does not change with varying DR height. The optimum DR height is found to be $0.32\lambda_g$. Once the height is identified, the exact frequency band at which the antenna yields broad beamwidth in two principle planes can be predicted. Next, critical step will be to successfully excite the desired broadside modes by choosing an optimum feed dimension and location. It is well known that in aperture-coupled CDRAs and RDRAs, broadside modes are excited when the slot is located below the central region of the DR [23]. Two important points need to be kept in consideration while feed dimensions are optimized; 1) to excite Mode-I and Mode-II, 2) to choose the dimensions so that modal resonance bandwidths are increased. This is achieved by increasing the slot width. It was found by simulations and experiments that the broadbeam frequencies occupy a band higher frequency part of Mode-I resonance bandwidth.

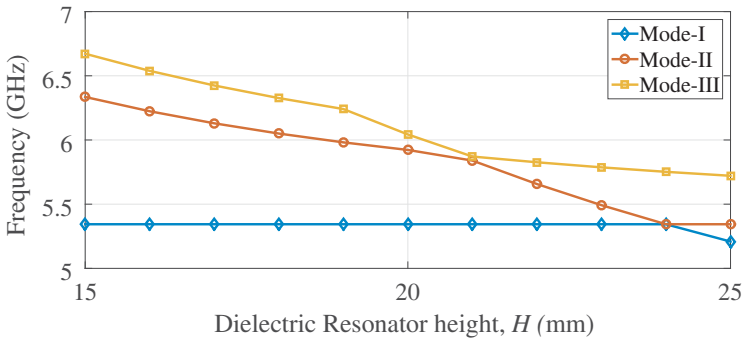

Figure 2. Mode frequencies of isolated CoP-RDR versus CoP-RDR height, *hdr*.

3.2. Mode Analysis

Figure 3 and Figure 4 show the vector field distributions inside the single element RDR and CoP-RDR at 5.5 GHz and 5.8 GHz, respectively. In Figure 3, it can be seen that the E-field configuration is of an azimuthal higher order mode owing to the presence of a full E-field cycle. This is identified as TE^{x}_{112} mode. The radiation from single element RDRA owes to this mode which alone yields a broad beamwidth in both principal planes but cannot enhance the beamwidth bandwidth. In Figure 4, however, there are

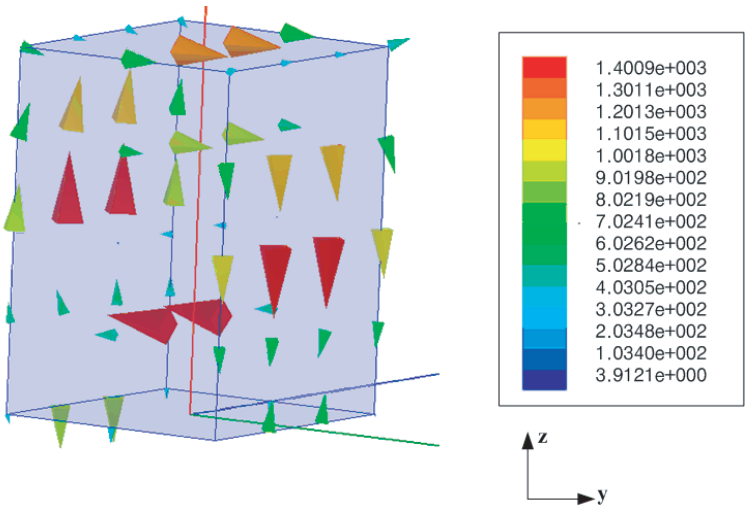

Figure 3. Vector field distribution inside single element RDR.

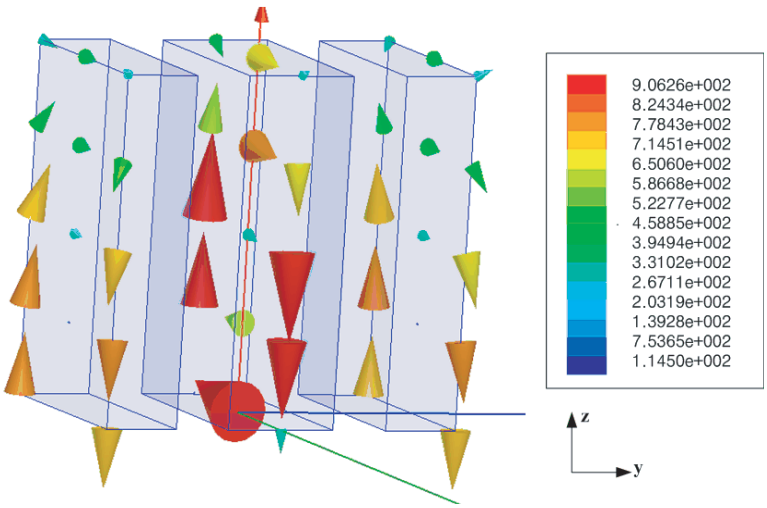

Figure 4. Vector field distribution inside CoP-RDR.

two E-field configurations seen simultaneously. A complete E-field cycle can be seen in the radiating element; alternatively it can be said that there are two E-field half cycles in the azimuthal direction, clearly implying that the mode is azimuthal higher order mode TE^x_{112}. The E-fields inside the parasitic dielectric elements, however, are induced fields suggesting that the mode is fundamental TE mode, i.e., TE^x_{111}. Therefore, in CoP-RDRA, there are two modes that are simultaneously excited owing to the presence of parasitic elements. It is due to these two broadside modes that the antenna yields broadbeam in two planes simultaneously and over a broader range of frequencies. Here it is vital to mention that initially the vertical gaps introduced were smaller, but as the design takes its final form through optimizations, the gap length increases to an extent that the side elements are no longer fed directly by the aperture slot, but they are parasitically fed by the main radiating element. Therefore, the antenna configuration is more of a coplanar parasitic form than just air gaps. Once the broadbeam band of frequencies is successfully enhanced by introducing parasitic DR elements, fine tuning of an important parameter can be even more lucrative towards achieving the goal. Gap length between the radiating element and parasitic elements is an important parameter that plays a vital role in enhancing the beamwidth bandwidth. Table 1 enlists E-plane and H-plane beamwidths at 5.5 GHz corresponding to various gap lengths. The effect of gap length on beamwidth bandwidth can also be observed from

Table 1. The E-plane and H-plane beamwidths at 5.5 GHz of CoPRDRA with various gap lengths.

Gap (mm)	E-plane HPBW	H-plane HPBW	Broadbeam band
0	139°	132°	5.3 GHz–5.5 GHz
0.5	136°	126°	5.4 GHz–5.6 GHz
1	135°	122°	5.4 GHz–5.7 GHz
1.5	130°	117°	5.5 GHz–5.7 GHz
2	128°	114°	5.5 GHz–6.0 GHz
3	122°	110°	5.5 GHz–6.1 GHz
4	118°	106°	5.6 GHz–6.1 GHz

the table entries in last column. An optimum gap length provides suitable coupling between radiating and parasitic DR elements.

Table 1 reveals two significant facts; as the gap increases, the frequency of operation and the broadbeam frequencies shift towards higher values, and the beamwidth bandwidth increases with larger gap. Furthermore, slight change in gap length affects the beam pattern, beamwidth, and frequency shift of the antenna.

Based on the above results, we summarize the steps for the design of broadbeam of CoP-RDRA. First calculate the estimated frequency using Eq. (1) for initial dimensions of RDR. Those dimensions and f_o may be used as initial values in eigen mode solver settings to find Mode-I frequency. Using this wavelength at this frequency (λ_g), aperture slot dimensions are calculated by $L_s = 0.203\lambda_g$ and $W_s = 0.115\lambda_g$. How slot dimensions are optimized will be shown in the next section. Also change the DR height H as $0.315\lambda_g$. This will result in a broadbeam single element RDRA and serve as a basis for the design of a broadbeam CoP-RDRA. Now, since the optimum DR height has been decided, one must calculate the widths of the main radiating and parasitic elements using $W_{\mathrm{DR}} = 0.107\lambda_g$ and $W_{\mathrm{PE}} = 0.0714\lambda_g$. Again using HFSS Eigen mode solver, simulate the radiating and parasitic element and get the value for Mode-I, Mode-II, and Mode-III frequencies. Now, λ_g value is to be updated using Mode-I frequency wavelength for CoP-RDR. Using the same relations for slot dimension and gap length, $g = 0.0535\lambda_g$ but with updated lambda and a few minor tweaks will yield a broadbeam CoP-RDRA.

4. ANTENNA PERFORMANCE

Parametric sweeps were run to optimize slot dimensions. Figure 5 and Figure 6 show various reflections coefficients with varying slot length and slot width, respectively. It is noted that when one parameter is varied, the other is kept constant. In order to get a broadbeam radiation pattern in two planes, it is imperative to make sure that Mode-I is excited and secondly that its modal resonance bandwidth is increased. From both the figures, it can be observed that as slot length is increased in length, Mode-I is strongly excited. Similarly, as slot width is increased again, the influence of Mode-I becomes stronger. From the parametric sweeps, it can be observed that when slot length and width reach the values of 11.5 mm and 6.5 mm, respectively, the 10 dB return loss or the reflection coefficient becomes most optimum. These slot dimensions are broader than those used typically to excite a mode, and the reason for this is that it helps increase the mode resonance bandwidth.

In order to validate simulated results of the proposed broadbeam CoP-RDRA, a prototype is fabricated and measured, shown in Figure 13. To fabricate the dielectric resonator structure $2 \times (2 \times 12 \times 18)$ mm thick off the shelf available ceramic slabs with dielectric constant of 9.8 were joined together with the help of adhesive to form one parasitic element (PE). Similar steps were repeated to form the second PE. For the radiating element, 3 slabs of same size were joined together. Gap length is maintain by filling a 3 mm thick foam with height and width same as those of dielectric resonators. The prototype reflection coefficient was measured with ANRITSU MS4644A VNA, and radiation patterns were measured in a state-of-the-art anechoic chamber. Single element RDRA and coplanar parasitic RDRA (with optimum gap length) both with height 18 mm were simulated to have a clear comparative understanding of the antenna responses. Figure 7 shows the simulated and measured

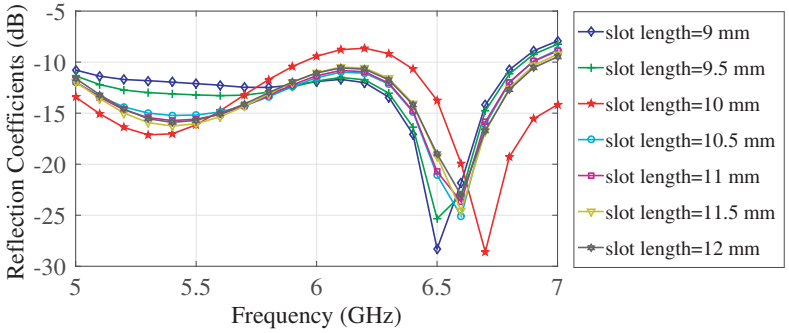

Figure 5. Reflection coefficients for various slot lengths.

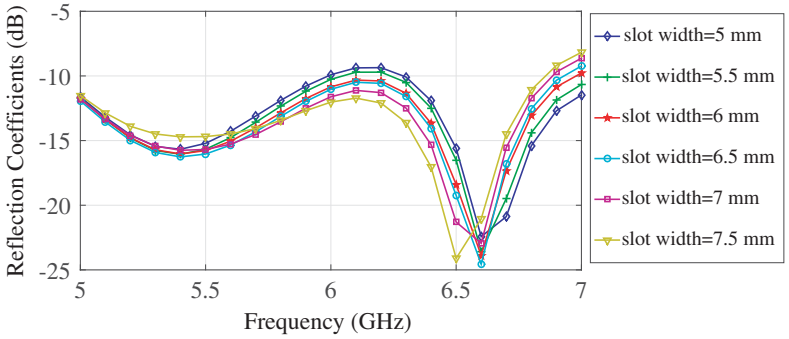

Figure 6. Reflection coefficients for various slot widths.

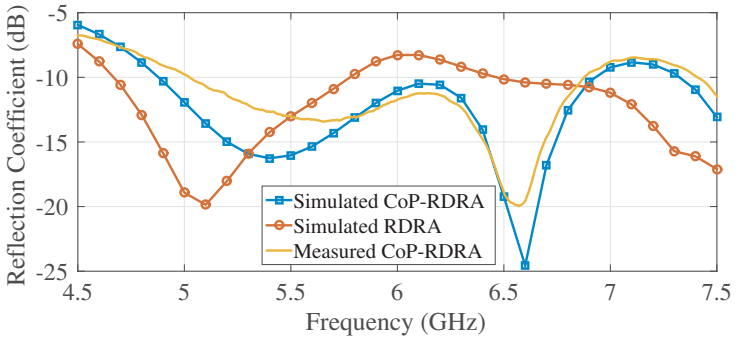

Figure 7. Simulated and measured reflection coefficients.

reflection coefficients of the CoP-RDRA as well as a comparison between the operating frequency bandwidths of single element RDRA and CoP-RDRA. It can be observed that the coplanar parasitic RDRA has broader operating frequency bandwidth than single element RDRA. It will be shown later that the beamwidth and beam pattern responses of the CoP-RDRA are also better than the single element RDRA. The simulated operating frequency bandwidth of coplanar parasitic RDRA is from 4.8 GHz to 6.9 GHz. The measured bandwidth is from 5.12 GHz to 6.83 GHz. It is revealed that the widest achievable bandwidth for single element RDRA is from 4.6 GHz to 5.7 GHz with beamwidth bandwidth being only 200 MHz, i.e., from 5.4 GHz to 5.6 GHz. However, the coplanar parasitic RDRA with optimum gap length of 3 mm yields frequency bandwidth of 2 GHz with broadbeam bandwidth of 700 MHz. Additionally, the beamwidths in both planes are uniform implying that the antenna illuminates the area above it uniformly.

Figure 8 shows the measured and simulated radiation patterns of the coplanar parasitic RDRA at 5.8 GHz. The measured and simulated patterns are quite in coherence. The simulated xoz beamwidth

at 5.8 GHz is 135°, and measured *xoz* beamwidth is 144°. The *yoz* simulated and measured beamwidths at 5.8 GHz are 117° and 116°, respectively. In addition, the cross polar patterns for both *xoz* and *yoz* patterns are 20 dB lower than the main beam. Figure 9 and Figure 10 show the simulated and measured

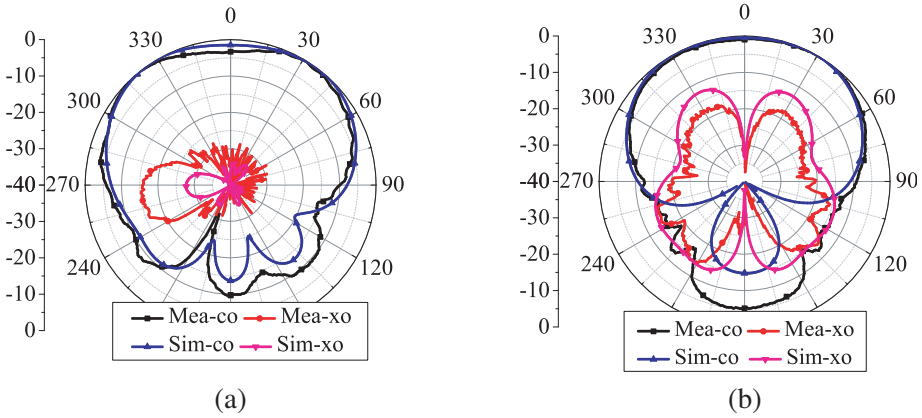

Figure 8. Simulated and measured radiation patterns of CoP-RDRA at 5.8 GHz, (a) *xoz*-pattern, (b) *yoz*-pattern.

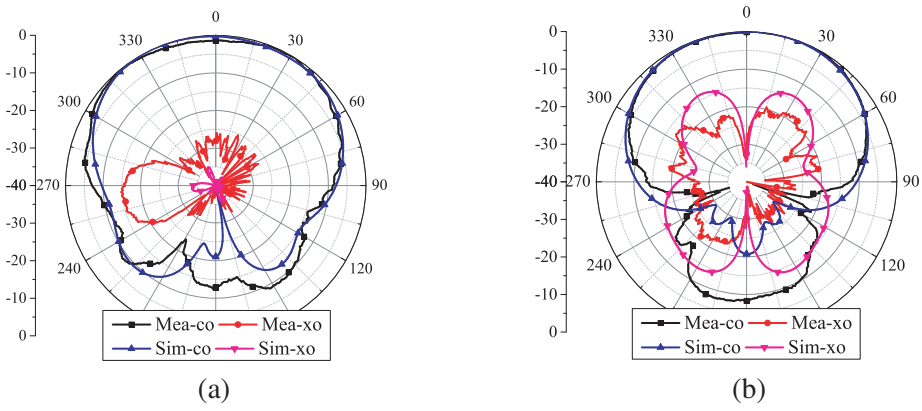

Figure 9. Simulated and measured radiation patterns of CoP-RDRA at 5.5 GHz, (a) *xoz*-pattern, (b) *yoz*-pattern.

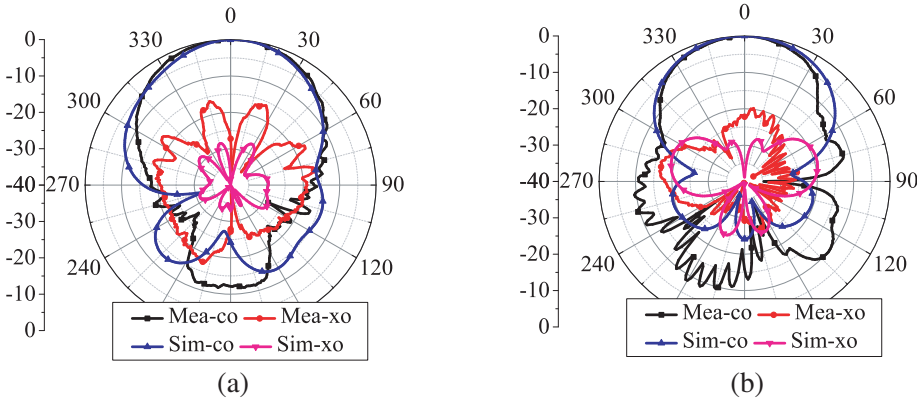

Figure 10. Simulated and measured radiation patterns of CoP-RDRA at 6.7 GHz, (a) *xoz*-pattern, (b) *yoz*-pattern.

radiation patterns at 5.5 GHz and 6.7 GHz, respectively. It is quite evident from radiation pattern figures that beamwidths in E- and H-planes at 5.5 and 5.8 GHz have wide half power beamwidths in both working planes simultaneously. However, radiation pattern at 6.7 GHz is clearly narrow beam in E- and H-planes since this frequency is out of broadbeam band of frequencies. Table 2 lists the simulated and measured beamwidths of CoP-RDRA and simulated beamwidths of single element RDRA. Table 3 compares the estimated beamwidths of prior literature with the proposed antenna. In any of the referenced papers, the beamwidths were not mentioned. 'NA' is mentioned where the antenna proposed in the paper does not yield a broadside radiation pattern. 'NM' is written where the radiation patterns have been neither presented nor mentioned in the paper. It is quite evident from this comparison that the proposed design yields wider beamwidths in both planes than all in the referenced literature. Figure 11 shows the xoz and yoz radiation patterns for a single element RDRA. It can be observed in Figure 11(a) that there is a dip at 0° which is 5 dB lower than the peak value in the radiation pattern. This suggests that the pattern contains out of phase components which inhibits it from yielding broadside pattern; on the contrary, the pattern may look and function like that of short vertical electric dipole. Figure 11(b) clearly shows that the copolar yoz pattern has high back lobe radiation which is approximately 4.5 dB lower than the main beam. The cross polar pattern is also high and is only 10 dB lower than the

Table 2. Comparison of beamwidths.

Frequency (GHz)	**Simulated**		**Measured**		**Single element**	
	E-plane	**H-plane**	**E-plane**	**H-plane**	**E-plane**	**H-plane**
5.4	117°	108°	115°	106°	127°	112°
5.5	123°	115°	115°	115°	146°	126°
5.6	127°	120°	124°	119°	147°	134°
5.7	131°	122°	129°	122°	59°	144°
5.8	134°	124°	127°	122°	66°	144°
5.9	138°	124°	130°	124°	147°	92°
6.0	142°	122°	142°	121°	98°	61°
6.1	146°	115°	144°	113°	48°	59°

Table 3. Comparison of beamwidths.

Frequency (GHz)	**Beamwidth**		**DRA Shape**	ϵ_{dr}	**Mode**
	xoz	yoz			
[12]	NA	NA	RDRA	10.2	$TE_{11\delta}$, $TE_{12\delta}$, $TE_{23\delta}$
[13]	NM	NM	RDRA	10.2	NM
[14]	$< 90°$	$< 100°$	RDRA	4.3	NM
[15]	$< 90°$	$< 90°$	RDRA	4.3 and 9.2	$TE^{y}_{1\delta1}$, $TE^{y}_{2\delta2}$, $TE^{y}_{1\delta3}$
[16]	120°	120°	RDRA		TE_{111}
[17]	$< 130°$	$< 100°$	CDRA	9.8	$HEM_{11\delta}$
[18]	$< 85°$	$< 85°$	CDRA	8.9	$HEM_{11\delta}$
[19]	$< 85°$	$< 85°$	CDRA	37	$HEM_{11\delta}$
[20]	$< 150°$	$< 80°$	CDRA	10	$HEM_{11\delta}$
[21]	$< 110°$	$< 85°$	CDRA	10	$HEM_{11\delta}$
[22]	$< 70°$	$< 80°$	CDRA	9.4	$HEM_{11\delta}$
	$< 105°$	$< 88°$			HEM_{113}
Broadbeam design	138°	122°	CoP-RDRA	9.8	TM_{111} TM_{112}

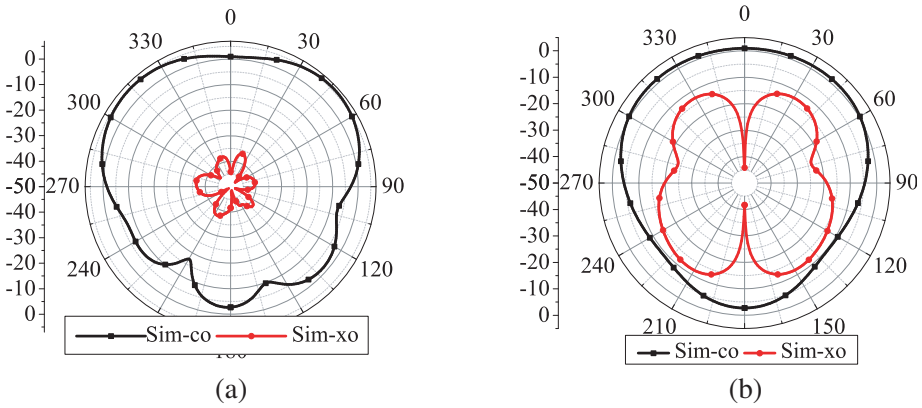

Figure 11. Simulated radiation patterns of single element RDRA at 5.8 GHz, (a) *xoz*-pattern, (b) *yoz*-pattern.

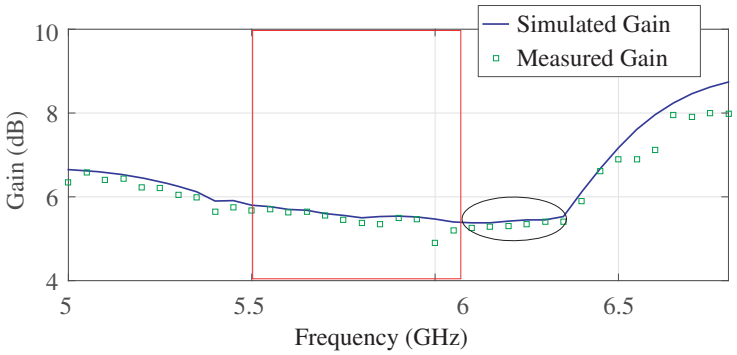

Figure 12. Simulated and measured gain.

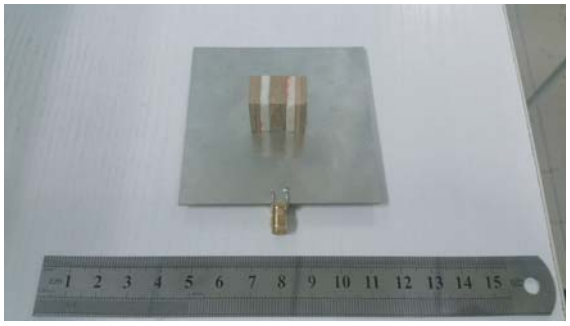

Figure 13. Photograph of antenna prototype.

main beam. The *yoz* beamwidth, however, is found to be 149°. Figure 12 shows the measured and simulated gain plots of the CoP-RDRA over the entire operational frequency bandwidth. It shows that in the fractional band at which the antenna exhibits broadbeam radiation pattern, and the gain is comparatively low and ranges from 5.5 dB to 6 dB. The red square region marks the frequency band (5.5 GHz to 5.8 GHz) at which the antenna yields wide beamwidth in *E*- and *H*-planes simultaneously, i.e., greater than 120° in both working planes. The frequency band marked in black eclipse region also shows a low gain because at these frequencies the antenna yields wide beamwidth only in *E*-plane. At frequencies higher than 6.35 GHz, the gain is high. The maximum simulated gain reaches up to 8 dB. Figure 14 shows the measured and simulated antenna efficiencies (%). It ranges from 82% to 87%.

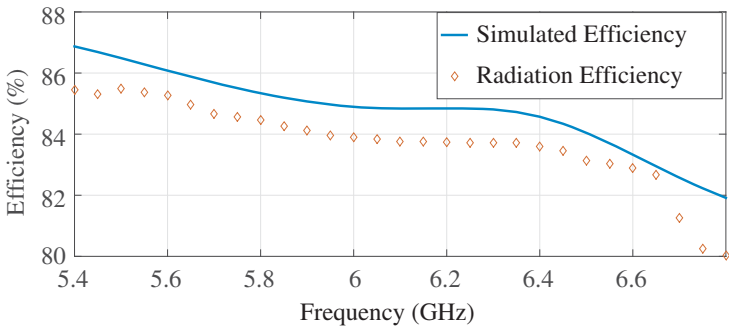

Figure 14. Antenna efficiency.

5. CONCLUSION

A novel broadbeam coplanar parasitic rectangular dielectric resonator antenna is presented in this paper. The proposed antenna consists of a main radiating dielectric resonator element and two parasitic elements which play an important role in conditioning the radiation pattern and improving the broadbeam bandwidth. Three modes are simultaneously excited inside the CoP-RDRA by only using a wide slot and not any additional feed mechanisms. However, first two modes are the desired modes which play a role in yielding broadbeam in two planes and enhancing broadbeam bandwidth. E-fields inside the parasitic elements are of fundamental TE^x_{111}, mode and that of radiating element are of TE^x_{112} mode. The CoP-RDRA is also compared with a single element RDRA, and the results clearly show that the latter has narrow impedance bandwidth and ripple in the E-plane radiation pattern, and the broadbeam bandwidth is narrow, i.e., 200 MHz.

ACKNOWLEDGMENT

The authors would like to thank Mr. Hongwei Yu, Mr. Yixuan Zhang and Mr. Zhendong Wang from Xidian University and Kangkang Han from Northwestern Polytechnic University, Xi'an, China for their time and guidance in antenna fabrication and measurement.

REFERENCES

1. Patel, R. and K. J. Han, "Utilization of higher-mode resonance in broadening the E-plane HPBW of printed antenna for automotive radar application," *Proc. Inter. Workshop Antennas Technology (iWAT)*, 330–332, Mar. 2015.
2. Mukherjee, B., P. Patel, and J. Mukherjee, "Hemispherical dielectric resonator antenna based on apollonian gasket of circles — A fractal approach," *IEEE Trans. Antennas Propag.*, Vol. 62, No. 1, 40–47, Oct. 2014.
3. Cheng, Y. F., X. Ding, W. Shao, M. X. Yu, and B. Z. Wang, "2-D planar wide-angle scanning-phased array based on wide-beam elements," *IEEE Antennas Wireless Propag. Lett.*, Vol. 16, 876–879, 2017.
4. Dadgarpour, A., B. Zarghooni, B. S. Virdee, and T. A. Denidni, "Single end-fire antenna for dual-beam and broad beamwidth operation at 60 GHz by artificially modifying the permittivity of the antenna substrate," *IEEE Trans. Antennas Propag.*, Vol. 64, No. 9, 4068–4073, Sep. 2016.
5. Zhang, J. W., S. S. Zhong, and Q. Wu, "Large-bandwidth patch antenna with ridge-shaped ground plate," *Microwave and Optical Technology Letters*, Vol. 48, No. 9, 487–488, Mar. 2006.
6. Chattopadhyay, S., J. Y. Siddiqui, and D. Guha, "Rectangular microstrip patch on a composite dielectric substrate for high-gain wide-beam radiation patterns," *IEEE Trans. Antennas Propag.*, Vol. 57, No. 10, 3325–3328, Oct. 2009.

7. Haidan, H., "A novel wide beam, circular polarization antenna — Microstrip-dielectric antenna," *Proc. Inter. Conf. Microwave and Millimeter Wave Technology (ICMMT)*, 381–384, Beijing, China, Aug. 2002.
8. Chang, T.-H. and J.-F. Kiang, "Dielectric resonator antenna with bending metallic planes," US patent, 2009/0102739 A1, 2008.
9. Hui, K. Y. and K. M. Luk, "A patch loaded dielectric resonator antenna," *Proc IEEE Region 10 Conf. (TENCON)*, 1–4, Melbourne, Australia, Nov. 2005.
10. He, Y., W. Wang, and X. Du, "A wide-band wide-beam dielectric resonator antenna," *Proc IEEE Conf. Antenna Measurements Applications (CAMA)*, 210–212, Tsukuba, Japan, Dec. 2017.
11. Luk, K. M. and K. W. Leung, *Dielectric Resonator Antennas*, Research Studies Press, London, UK, 2011.
12. Kiran, D. V., D. S. Narayanan, V. K. Killamsetty, and B. Mukherjee, "Photonic waveguide inspired corrugated cross-coupled notch DRA," *Electromagnetics, Taylor & Francis*, Vol. 38, No. 7, 458–468, Aug. 2018.
13. Patel, B. A., V. B. Vaghela, and H. Patel, "Design and simulation of rectangular dielectric resonator antenna for UWB application," *IJSRD — International Journal for Scientific Research & Development*, Vol. 3, No. 03, 711–713, 2015.
14. Kshirsagar, P., S. Gupta, and B. Mukherjee, "Novel design of conformal-strip excited asymmetrical rectangular dielectric resonator antenna for ultra-wide band application," *Journal of Microwave Power & Electromagnetic Energy, Taylor and Francis*, Vol. 52, No. 2, 128–141, 2018.
15. Kshirsagar, P., S. Gupta, and B. Mukherjee, "A two segment rectangular dielectric resonator antenna for ultra-wideband application," *Electromagnetics, Taylor & Francis Electromagnetics, Taylor and Francis*, Vol. 38, No. 1, 20–33, 2018.
16. Kajfez, D., A. W. Glisson, and J. James, "Evaluation of modes in dielectric resonators using a surface integral equation formulation," *Proc. IEEE MTT-S Inter. Microwave Symposium Digest*, 409–411, Boston, MA, USA, 1983.
17. Gupta, P., D. Guha, and C. Kumar, "Dielectric resonator working as feed as well as antenna: New concept for dual-mode dual-band improved design," *IEEE Trans. Antennas Propag.*, Vol. 64, No. 4, 1497–1502, Jan. 2016.
18. Deng, L., M. Seltzer, and D. Yu, "Characteristics of aperture-coupled cylindrical dielectric resonator antennas on a thick ground plane," *IEE Proceedings — Microwaves, Antennas and Propag.*, Vol. 146, No. 6, 439–442, Dec. 1999.
19. Junker, G. P., A. A. Kishk, and A. W. Glisson, "Input impedance of dielectric resonator antennas excited by a coaxial probe," *IEEE Trans. Antennas Propag.*, Vol. 42, No. 7, 960–966, Jul. 1994.
20. Leung, K. W. and S. K. Mok, "Circularly polarized dielectric resonator antenna excited by a perturbed annular slot with a backing cavity," *Electronics Lett.*, Vol. 37, No. 15, 934–936, Jul. 2001.
21. Guha, D., P. Gupta, and C. Kumar, "New mode in dielectric resonator antenna with strawberry shaped radiations covering a wide beamwidth," *Proc. Inter Symposium Antennas Propag. and USNC-URSI Radio Science Meeting (APSURSI)*, 1912–1913, 2013.
22. Gupta, P., D. Guha, and C. Kumar, "Dielectric resonator working as feed as well as antenna: New concept for dual-mode dual-band improved design," *IEEE Trans. Antennas Propag.*, Vol. 64, No. 4, 1497–1502, Jan. 2016.
23. Simons, R. N. and R. Q. Lee, "Effect of parasitic dielectric resonators on CPW/aperture — Coupled dielectric resonator antennas," *IEE Proc. Part H*, Vol. 140, No. 5, 336–338, Oct. 1993.